MOLECULAR DYNAMICS AND HEAD–TAIL DISORDER IN THE RAMAN SPECTRUM OF CRYSTALLINE N_2O ☆

Gianni CARDINI, Giorgio F. SIGNORINI, Pier R. SALVI and Roberto RIGHINI
Department of Chemistry, University of Florence, Via G. Capponi 9, 50121 Florence, Italy

Received 4 August 1987; in final form 23 October 1987

The effect of head–tail disorder on the low frequency Raman spectrum of solid N_2O is investigated by means of molecular dynamics simulations. The main features of the experimental spectrum are reproduced in the calculation under the assumption that about 10% of the molecules are orientationally disordered.

1. Introduction

The dynamics of molecular crystals of diatomic and small linear molecules belonging to the cubic system, such as N_2, CO CO_2, N_2O, have been extensively studied, both from the theoretical and the experimental points of view. N_2 [1–5] and CO [2,6] are known as typical anharmonic crystals, characterized by large librational amplitudes and broad phonon linewidths at very low temperature [4–6]; both crystals undergo solid-state phase transitions to disordered structures. In this respect CO_2 and N_2O behave quite differently: the molecular librational amplitudes are in fact rather small [2,7], and their anharmonicity is definitely low. Only one solid phase is known for both crystals under normal pressure. In CO and N_2O crystals, the lack of molecular inversion symmetry allows two possible orientations of the molecular dipoles parallel to the body diagonals of the unit cell; in fact, both crystals are characterized by a certain degree of orientational disorder [8–13]. Solid N_2O is known to be orientationally disordered at low temperature from the early calorimetric work by Giauque et al. [9]. Several papers have been published to clarify the mechanism of the molecular reorientation and to asses the actual degree of disorder in such crystals. Thermodynamic [10], dielectric [11], electron [12] and neutron [13] diffraction data have been utilized, leading to the conclusion that the large orientational disorder of solid N_2O near the melting point is almost completely frozen-in when the temperature is lowered [11]. On the other hand, the rate of molecular reorientation at low temperatures is negligible [11]. In this respect, N_2O differs substantially from CO crystals which are characterized by molecular flipping at very low temperatures [8].

The experimental phonon spectra of solid N_2O have been interpreted on the basis of the T_h^6 space group, corresponding to a fully disordered crystal [14]. In contrast, the harmonic lattice dynamics calculations published up to now [14,15] have necessarily been based on a perfectly ordered T_4 structure. The good agreement between experiment and theory is actually not surprising, in view of the very small molecular dipole and the similarity of the oxygen and nitrogen interaction potentials: randomizing the molecular orientations then results in a minor perturbation of solid N_2O. However, although the phonon frequencies are apparently unaffected by the crystal disorder, the same does not necessarily hold for the phonon lineshapes. We have thus investigated the low-frequency Raman spectrum of solid N_2O at low temperature and compared the experimental lineshapes with the spectra calculated from molecular dynamics and anharmonic lattice dynamics, in order to clarify the effects of molecular disorder on the linewidths and lineshapes of the phonon spectra.

☆ Work supported by the Italian MPI and CNR.

2. Raman spectrum

The Raman spectrum of solid N_2O has been published by Anderson and Sun [15]. However, since the shape of the phonon bands is the main interest of the present work, we re-measured the spectrum in the low-frequency region at 10 K. The sample was deposited from the vapour on a cold finger and annealed repeatedly at 80 K. The good resolution of the factor group and LO–TO components of ν_1 was taken as a check of the complete crystallization of the sample. The frequencies of the spectrum shown in fig. 1 coincide with those of ref. [15]. Not surprisingly, the peak positions are very close to those observed in the corresponding spectrum of solid CO_2 [16]: the cell dimension, the molecular mass, the moment of inertia and the intermolecular forces are in fact similar in the two crystals. In contrast, the lineshapes of the band in fig. 1 differ substantially from those of carbon dioxide: the phonon lines of crystalline CO_2 at low temperatures are in fact very narrow (at 5 K they are 0.12, 0.24 and 1.5 cm^{-1}, with increasing frequency [16,17]). The N_2O spectrum on the other hand shows quite broad lines, with linewidths much larger than the instrument resolution (1 cm^{-1}); more surprisingly, the linewidths do not increase with the phonon frequency (following the pattern of the two-phonon density of states) as observed in several other cases [5–7]. The broadest band in fact corresponds to the phonon at 70.5 cm^{-1}; in our spectrum this band clearly shows an asymmetry on the low frequency side, although we did not observe the well-defined shoulder at about 66.5 cm^{-1} reported by Anderson and Sun [15]. Such a difference suggests that the intensity of this spectral feature could be related to the size of the microcrystallites of the sample and to the annealing procedure.

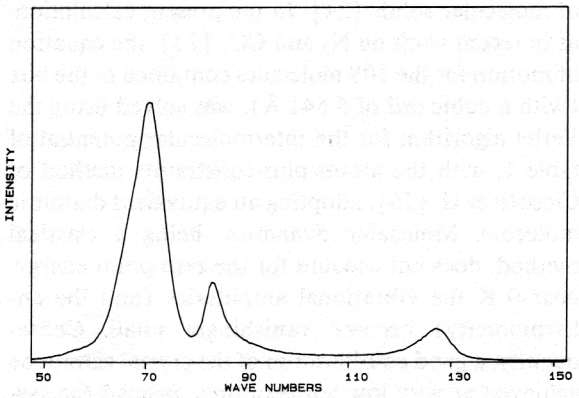

Fig. 1. Raman spectrum of solid N_2O measured at 10 K.

3. Lattice dynamics (LD) calculation

The ordered T_4 structure was adopted for the LD calculation.

A atom–atom plus charge–charge interaction potential was used for the calculation of the phonon spectrum of solid N_2O. The potential parameters, collected in table 1, were obtained by fitting to the harmonic $\boldsymbol{k}=\boldsymbol{0}$ lattice frequencies, to the lattice energy and to the unit cell dimension, as shown in table 2. The molecular dipole reproduces the experimental value [21]. The quadrupole moment adopted in the present model is larger than the value of 3×10^{-26} esu recommended in ref. [22]; in ref. [11] an even larger value (5.1×10^{-26} esu) was adopted in the potential used for the calculation of the linewidths of librons in N_2O. A similar value was chosen in a recent calculation of phonon linewidths in CO_2 [7], where a quadrupole moment of 4.3×10^{-26} esu was used, 25% larger than the experimental value. In both cases a large electrostatic contribution is required to keep the anharmonicity of the potential model reasonably low. In fact, as is shown in ref. [7], the an-

Table 1
Intermolecular potential for solid N_2O. (A) Atom-atom potential: $V=4\epsilon[(\sigma/r)^{12}-(\sigma/r)^6]$. (B) Electrostatic potential $V=q_iq_j/r$ (units of electron charge)

	Contact	ϵ (K)	σ (Å)
A	N–N	51.83	3.252
	N′–N	39.25	2.967
	N′–N′	–	–
	N–O	48.81	3.031
	N′–O	54.85	3.081
	O–O	74.98	3.230
	the interaction centers are placed on the nuclei; N′ is the central atom		
B	$q(N)=-0.3665$		
	$q(N')=0.6858$		
	$q(O)=-0.3193$		
	molecular dipole $\mu=0.166\times10^{-18}$ esu		
	molecular quadrupole $q=4.426\times10^{-26}$ esu		

Table 2
Lattice frequencies and linewidths (cm^{-1}) of N_2O

Species		Exp. ω		LD calculation			
T_4	T_h^6			ω	intensity [e]		2Γ
					IR	Raman	
T	T_g	126.5 [a]	125 [b]	127.7	0.9	4.5	6.7
T	T_u		118 [b]	113.0	100	2.0	7.2
E	E_u			92.9	–	3.0	2.5
T	T_g	83.0 [a]		86.0	6.6	30	1.5
A	A_u			81.4	–	–	0.4
T	T_u	(66.5 [a])	68 [b]	75.1	43	0.4	0.8
E	E_g	70.5 [a]		67.2	–	100	0.4
$E_{lattice}$			−24.2 [c]	−23.8			
unit cell (Å)			5.641 [d]	5.63			

[a] Present work at 10 K and ref. [15] at 18 K. [b] Ref. [18], at 1.8 K. [c] Ref. [10] (in kJ/mol). [d] Ref. [19].
[e] Calculated according to ref. [20].

harmonic terms of the potential expansion are dominated by the atom–atom part. In this respect, the quadrupole used here should be taken as an effective value.

The choice of different sets of potential parameters for the two nitrogen atoms (corresponding to the different electron density distribution around the nuclei) gave us a much better fit of the experimental data; for simplicity, the interaction between the two central atoms was not included, since it has practically no effect on the dynamics of the crystal, and gives only a minor contribution to the lattice energy.

The same potential and structure were used to calculate the phonon linewidths; the theory of anharmonic lattice dynamics and the method of calculation have been described in several articles and books [23], and will not be given here. The linewidths of the $\boldsymbol{k}=\boldsymbol{0}$ phonons were calculated according to the expression

$$\Gamma_j(\Omega) = 18\hbar^{-2}\sum_{\boldsymbol{k}}\sum_{j_1 j_2}\left|B\begin{pmatrix} j & j_1 & j_2 \\ 0 & k & -k \end{pmatrix}\right|^2$$
$$\times\{(\bar{n}_{j_1 k}+\bar{n}_{j_2 k}+1)[\delta(\Omega-\omega_{j_1}(\boldsymbol{k})-\omega_{j_2}(\boldsymbol{k}))$$
$$-\delta(\Omega+\omega_{j_1}(\boldsymbol{k})+\omega_{j_2}(\boldsymbol{k}))]$$
$$+(\bar{n}_{j_1 k}-\bar{n}_{j_2 k})[\delta(\Omega+\omega_{j_1}(\boldsymbol{k})-\omega_{j_2}(\boldsymbol{k}))$$
$$-\delta(\Omega-\omega_{j_1}(\boldsymbol{k})+\omega_{j_2}(\boldsymbol{k}))]\}, \qquad (1)$$

where B are the cubic anharmonic coefficients calculated from the potential in table 1, ω are the harmonic frequencies and n are the thermally averaged occupation numbers.

The calculated linewidths at 10 K are shown in table 2. Their values follow the same pattern (2Γ increasing with the phonon frequency) as that observed in the CO_2 crystal, in full contrast with the experimental data for N_2O (see fig. 1).

4. Molecular dynamics (MD) simulation

It has long been appreciated that MD can be utilized to investigate the lineshapes of phonon spectra of molecular solids [24]. In the present calculation, as in recent work on N_2 and CO_2 [25], the equation of motion for the 108 molecules contained in the box (with a cubic cell of 5.641 Å), was solved using the Verlet algorithm for the intermolecular potential of table 1, with the atoms-plus-constraints method of Ciccotti et al. [26], adopting an equivalent diatomic molecule. Molecular dynamics, being a classical method, does not account for the zero-point energy; near 0 K the vibrational amplitudes (and the anharmonicity) become vanishingly small. Consequently, a good equilibration of the crystal cannot be achieved at very low temperatures; instead the system was equilibrated for several thousand time steps

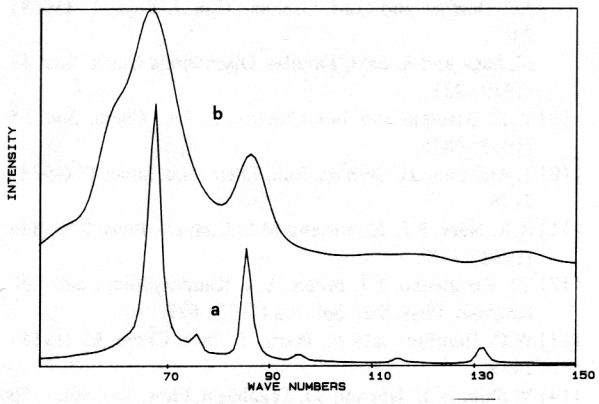

Fig. 2. (a) MD calculated Raman spectrum for a fully ordered sample of N_2O at 20 K. The actual linewidths are below the resolution of the calculation method (see text). (b) MD calculated Raman spectrum for a partially disordered sample of solid N_2O at 20 K (see text). A Gaussian smoothing with $\sigma = 2.0$ cm^{-1} has been applied.

(5×10^{-15} s each) at a temperature of about 40 K, and then cooled down to 20 K. All our MD results refer to this temperature. As expected, at 20 K no molecular flip was observed during the runs (typical length 61.5 ps).

The Raman spectrum was calculated from the anisotropic part of the crystal polarizability, stored at each time step:

$$\alpha_{ij}(t) \propto \sum_m r_{im}(t) r_{jm}(t) , \qquad (2)$$

where r_{im} is the ith component of the orientation vector of the mth molecule. According to eq. (2), only autocorrelation terms are included, and the oriented gas approximation is assumed. The Raman spectrum is finally obtained as the Fourier transform of the time-correlation function of $\alpha_{ij}(t)$ [27].

Two different simulation runs were performed. In the first (a), a starting configuration corresponding to the perfectly ordered T_4 structure was adopted. The Raman spectrum obtained at 20 K is shown in fig. 2a. Narrow lines are observed, in agreement with the prediction of anharmonic LD (see table 2). The lineshapes of the two bands at 68 and 86 cm^{-1} are actually limited by the "instrument" resolution: the intrinsic resolution of the calculation (0.8 cm^{-1}) due to the finite length of the time correlation, is lowered by the Gaussian smoothing ($\sigma = 0.6$ cm^{-1}) applied to the calculated spectrum. The weak bands that appear at about 75, 95 and 116 cm^{-1} correspond to mainly translational modes (see the LD calculated frequencies and intensities in table 2), which are Raman active according to T_4 symmetry. Such weak bands are not observed in the experimental spectrum, although the non-zero background seen in the 90–120 cm^{-1} region can be attributed to the scattering from weak and very broad transitions.

In the second calculation (b), a partially disordered starting configuration was obtained by 180° rotation of a fraction of the 108 molecules, randomly chosen. Following the same procedure as above, the Raman spectrum at 20 K was calculated for the disordered crystal. Fig. 2b shows the result for a sample containing 12 out of 108 molecules flipped. The effect of disorder on the lineshapes is dramatic: the lowest line broadens substantially, and a low frequency shoulder appears. The highest frequency band is also broadened and shifted to higher frequency, while the effect is much lower for the phonon at about 85 cm^{-1}. Such behaviour is in close agreement with the experimental spectrum in fig. 1.

5. Conclusion

The results of the MD similation, compared with anharmonic lattice dynamics and with the experimental spectrum, show that the orientational disorder of solid N_2O is responsible for the peculiar features in the Raman spectrum of this crystal. A relatively small proportion of flipped molecules (about 10%) is sufficient to substantially modify the lineshapes of the external phonons. Fig. 3 shows an analysis of the distribution of flipped molecules among the twelve first neighbours of each molecule in the sample utilized for simulation (b): about 75% of the molecules "see" at least one flipped molecule in their closest neighbour shell. It should be noted that the present results refer to a single disordered configuration; different random distributions of the same number of flipped molecules could possibly give different spectra, although we believe that the main features would be unchanged. This last aspect, together with the effects of increasing the temperature, and extension to a constant-pressure simulation will be the subject of future work.

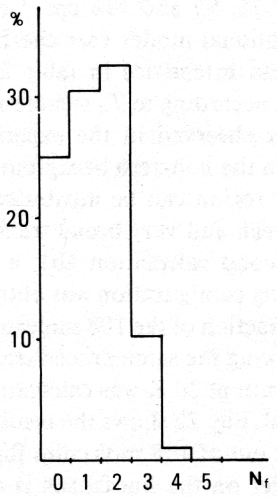

Fig. 3. Distribution of flipped molecules among the 12 first neighbours for all 108 molecules in the simulation box. The histogram shows the fraction (%) of the molecules that "see" a given number (N_f) of flipped molecules in the nearest neighbour shell.

References

[1] P.V. Dunmore, Can. J. Phys. 55 (1977) 554.
[2] T.N. Antsygina, V.A. Slusonov, Yu.A. Freiman and A.I. Eremburg, J. Low Temp. Phys. 56 (1984) 331.
[3] W.J. Briels, A.P.J. Jansen and A. van der Avoird, J. Chem. Phys. 81 (1984) 4118.
[4] K. Kobashi, Mol. Phys. 36 (1978) 225.
[5] G. Signorini, P.F. Fracassi, R. Righini and R.G. della Valle, Chem. Phys. 100 (1985) 361.
[6] P.F. Fracassi, R. Righini, R.G. della Valle and M.L. Klein, Chem. Phys. 96 (1985) 361.
[7] P. Procacci, R. Righini and S. Califano, Chem. Phys. 116 (1987) 171.
[8] J.O. Clayton and W.F. Giauque, J. Am. Chem. Soc. 54 (1932) 2610;
E.K. Gill and J.A. Morrison, J. Chem. Phys. 45 (1966) 1985;
J.C. Burford and G.M. Graham, Can. J. Phys. 47 (1969) 23;
H. Suga and S. Seki, Faraday Discussions Chem. Soc. 69 (1980) 221.
[9] W.F. Giauque and J.O. Clayton, J. Am. Chem. Soc. 55 (1933) 4875.
[10] T. Atake and H. Chihara, Bull. Chem. Soc. Japan 47 (1974) 2126.
[11] K.R. Nary, P.L. Kuhns and M.S. Conradi, Phys. Rev. B26 (1982) 3370.
[12] S.I. Kovalenko, E.I. Indan, A.A. Khudotyoplaya and I.N. Krupskii, Phys. Stat. Sol. 20a (1973) 629.
[13] W.C. Hamilton and M. Petrie, J. Phys. Chem. 65 (1961) 1453.
[14] Y. Shibata, K. Ishi and S.I. Takahashi, Phys. Stat. Sol. 135b (1986) 85.
[15] A. Anderson and T.S. Sun, Chem. Phys. Letters 8 (1971) 537.
[16] J.W. Schmidt and W.B. Daniels, J. Chem. Phys. 73 (1980) 4848.
[17] R. Ouillon, P. Ranson and S. Califano, J. Chem. Phys., to be published.
[18] K. Ishi, J. Phys. Soc. Japan 55 (1986) 384.
[19] I.N. Krupskii, A.I. Prokhvatilov and A.I. Erenburg Fiz. Nizk. Temp. 6 (1980) 1174.
[20] V. Schettino and S. Califano, J. Chim. Phys. 76 (1979) 197.
[21] M.W. Melhuish and R.L. Scott, J. Phys. Chem. 68 (1964) 2301.
[22] D.E. Strogryn and A.P. Strogryn, Mol. Phys. 11 (1966) 371.
[23] S. Califano, V. Schettino and N. Neto, Lecture notes in chemistry, Vol. 21. Lattice dynamics of molecular crystals (Springer, Berlin, 1981), and references therein.
[24] J.J. Weis and M.L. Klein, J. Chem. Phys. 63 (1975) 2869.
[25] G. Cardini and S.F. O'Shea, Phys. Rev. B32 (1985) 2489;
G. Cardini, P. Procacci and R. Righini, Chem. Phys. 117 (1987) 335.
[26] G. Ciccotti, M. Ferrario and J.P. Ryckaert, Mol. Phys. 47 (1982) 1253.
[27] B.J. Berne and R. Pecora, Dynamic light scattering (Wiley, New York, 1976).